Investigation of process parameters assessment *via* Design of Experiments for CO_2 photoreduction in two photoreactors

Alberto Olivo[1,2], Warren Athol Thompson[3], Elizabeth Rose Bache Bay[3], Elena Ghedini[2], Federica Menegazzo[2], M. Mercedes Maroto-Valer[3] Michela Signoretto[2,]*

[1] Low Emission Resources Corporation, 2 Mid Craigie Rd, Dundee, DD4 7RH, UK

[2] CatMat Lab, Dept. of Molecular Sciences and Nanosystems, Ca' Foscari University Venice and Consortium INSTM, RU of Venice, Via Torino 155, 30172 Venezia, Italy

[3] Research Centre for Carbon Solutions (RCCS), School of Engineering & Physical Sciences, Heriot-Watt University, Edinburgh, EH14 4AS, UK

**Corresponding Author: Prof. Michela Signoretto (miky@unive.it);*

Abstract:

CO_2 photoreduction with water to obtain solar fuels is one of the most innovative and sustainable processes to harvest light energy and convert it into hydrocarbons. Although photocatalytically active materials and photoreactors have been developed for this purpose, lack of standardisation in testing conditions makes the assessment of process parameters and the comparison of material performance a challenge. Therefore, this paper is aimed at investigating the effect of CO_2 photoreduction parameters irradiance and reaction time on production of methane from two photocatalytic rigs. This was pursued through a design of experiments (DOE) approach, which assessed the influence of experimental conditions between different setups. Using low irradiance (40 – 60 $W \cdot m^{-2}$), reaction time and temperature significantly affected methane production, with a maximum production of 28.50 $\mu mol \cdot g_{cat}^{-1}$ (40 $W \cdot m^{-2}$, 4 h). When using high irradiance (60 – 2400 $W \cdot m^{-2}$), only irradiance was found to significantly affect methane production, with a maximum production of $1.90 \cdot 10^{-1}$ $\mu mol \cdot g_{cat}^{-1}$ (1240 $W \cdot m^{-2}$, 2 h). Considering proposed reaction mechanism for CO_2 photoreduction, this paper highlights that experimental results give different yet complementary information on the two most important steps of the process, i.e. photoexcitation and surface chemical reaction.

Keywords: CO_2 photoreduction, titanium dioxide, process design, Design of Experiments

1 Introduction

Photoreduction is one of the most innovative, environmentally sustainable and promising technologies to convert carbon dioxide (CO_2) into hydrocarbons using water as a reducing agent and light as primary energy input [1, 2]. Efforts have been placed on researching how to improve the effectiveness of this process [1, 3, 4]. For example, photocatalysts modification is one of the pursued strategies, where several semi-conductors have been investigated, including CdS [5-7], ZnO [8-9], ZrO_2 [10], WO_3 [11], $SrTiO_3$ [12], although TiO_2 remains the most investigated and promising material [13-15]. Another strategy to increase photoactivity is materials modification, aimed at suppressing electron-hole recombination, which can be pursued in several ways: use of co-catalyst [16-19], metal doping [20], graphene encapsulation [21]; but one of the most promising options is the introduction of surface plasmonic resonance particles [21-24]. Material engineering aside, reactor design and catalytic conditions for CO_2 photoreduction still need to be further investigated and standardised to compare materials photoactivity significantly. A wide variety of photocatalytic reactors has been reported [25, 26, 27], but due to a lack in standardisation in experimental procedures, reaction regimes and data collection and processing, it is difficult to compare results reported from different systems. Recently, gas phase systems have been preferred to liquid phase to overcome limitations by photon and mass transfer [27, 28, 29], focusing on gas phase systems operating at room temperature and atmospheric pressure [30-32]. A recent study reported that when reagents are in gas phase, CO_2 undergoes deoxygenation faster than hydrogenation, improving selectivity to methane (CH_4), which is the most desired solar fuel, due to its high hydrogen to carbon ratio [28].

In the field of CO_2 photoreduction, general catalysis parameters (e.g. catalyst amount, reaction time, reagents concentrations) have been investigated [33-35], whilst photons irradiation, which represents the primary energy input have not been thoroughly studied yet. Materials light harvesting considerably affects surface activation and, consequently, the number of active sites to catalyse CO_2 photoreduction [36]. In the case of photooxidation reactions, correlation between photons input and reaction rate varies with photons flux, indicating different activation mechanisms [37]. However, to the best of the

authors' knowledge, photons input effect on CO_2 photoreduction with water has not been investigated yet.

In this paper, the authors investigate the effect of reaction time and irradiance on conversion. The choice of these parameters is due to their correlation to photons input in the catalytic system, which is the energy source of the whole process [38]. To provide a rational approach to understanding the effect of these parameters on CO_2 photoreduction into methane, a Design of Experiments (DOE) was employed for the first time for two different reactor designs. DOE is a powerful tool that allows for generating highly efficient systematic experimental designs that can be used to screen and optimise parameters on selected responses [39-41]. The objective of DOE is to fit a function including only statistically significant parameters to a response. The systematic treatment of the data employed here allows for parameters irradiance and reaction time to be compared for the two studied different reactor systems on the responses to methane production. This study highlights how reactor design and experimental conditions can affect selectivity and conversion in CO_2 photoreduction.

2 Experimental

2.1 Materials synthesis

Titanium dioxide was prepared by the precipitation method [28]. A 1.2 M titanyl sulphate solution ($TiOSO_4 \cdot xH_2O \cdot yH_2SO_4$, Ti assay > 29 % Sigma Aldrich) and a 9.0 M NaOH solution (assay > 97% Carlo Erba) were dropped simultaneously to 200 mL of distilled water under vigorous stirring, maintaining pH neutral. The $Ti(OH)_4$ suspension was then aged at 60 °C for 20 h, filtered and washed with distilled water to remove the sulphate ions, as verified by the barium chloride test [42]. Wet $Ti(OH)_4$ was dried at 110 °C for 18 h and finally calcined at 400 °C for 4 h in air flow to obtain TiO_2.

To introduce gold nanoparticles, the deposition–precipitation (DP) method was used since it allows to obtain small gold nanoparticles [43, 44]. Titanium dioxide was suspended in an aqueous solution of $HAuCl_4 \cdot 3H_2O$ for 3 h, maintaining pH at 8.6 by the addition of 0.5 M NaOH. Gold loading was 0.2 wt. %, as confirmed by flame atomic absorption spectrometry (FAAS). After filtration, the sample was washed from chlorides with distilled water, as verified by the silver nitrate test [45]. The wet catalyst was dried at 35 °C for 18 h and finally calcined in air for 1 h at 400 °C.

2.2 Characterization of the photocatalysts

N_2 adsorption–desorption isotherms at 196 °C were performed using a MICROMERITICS ASAP 2000 analyser to obtain information on the porous texture. All samples were previously outgassed at 200 °C for 2 h. The mesoporous volume was measured as the adsorbed amount of N_2 after capillary condensation. The surface area was evaluated using the standard BET [46] equation and the pore size distribution was obtained using the BJH method applied to the isotherm desorption branch [47].

X-ray diffraction (XRD) analyses were conducted using a Bruker Nonius X8-Apex2 CCD diffractometer with an Oxford Cryosystems Cryostream routinely running at 100K (copper anode; operating conditions, 40 kV and 40 mA) and a Si(Li) solid state detector (Sol-X) set to discriminate the Cu Kα radiation. Apertures of divergence, receiving and detector slits were 2.0 mm, 2.0 mm, and 0.2 mm, respectively. Data scans were performed in the 2θ range 5°–80° with 0.02° step size and counting times of 3 s/step. The actual amount of copper and gold loaded in the promoted catalysts was determined by flame atomic absorption spectroscopy (FAAS) using a PerkinElmer Analyst 100.

The UV-adsorption and bandgap of the coated glass slides were characterized by a UV/Vis spectrometer (Perkin Elmer lambda 950) equipped with a 150 mm integration sphere (Perkin Elmer). The band gap energy (BG) of the catalysts were determined by the intercept of a linear fit to the absorption edge and calculated according to Equation 1:

$$\mathrm{BG} = h \cdot \frac{c}{\lambda}$$

Equation 1

where: h is Planck's constant ($6.626 \cdot 10^{-34}$ $m^2 \cdot kg \cdot s^{-1}$), c is the speed of light ($3.00 \cdot 10^8$ $m \cdot s^{-1}$) and λ is the wavelength of adsorption.

2.3 Photoactivity tests at low irradiance

The catalytic apparatus used for the photoactivity tests at low irradiance is similar to that reported previously [28]. CO_2 photoreduction was carried out in a borate glass thin film reactor (length 33 mm, height 18 mm, thickness 2 mm). The catalyst (10 mg) was introduced by depositing a catalyst suspension in 2-propanol on the light-exposed side of the reactor.

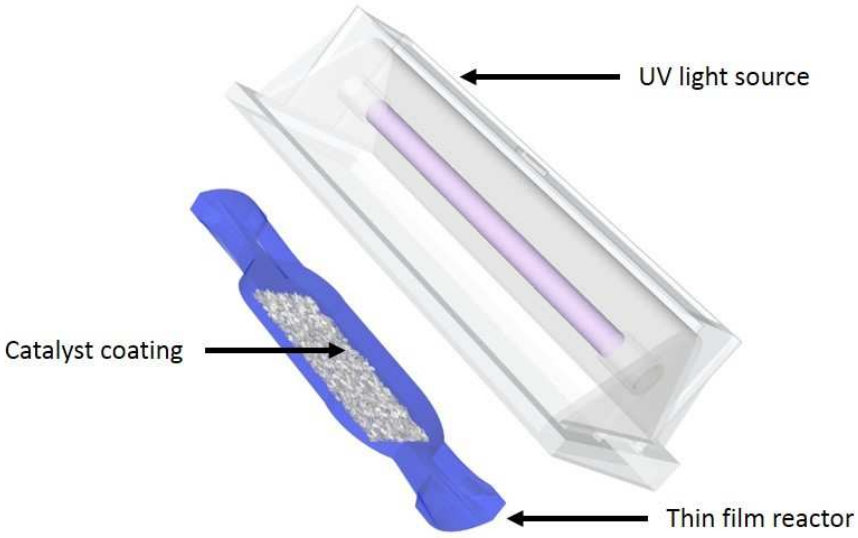

Figure 1 *Film reactor in light blue showing catalyst loaded and the light source housing and source purple.*

The samples were illuminated using a 125 W mercury UVA lamp (provided by Helios Italquartz srl, emission range 315–400 nm shielded by a special tubular quartz to select the 366 nm wavelength). It was measured with a photoradiometer (Delta OHM HD2102.2) that irradiance on illuminated surface of the reactor is the same on that behind irradiation source: thus it is possible to state that the reactor walls do not adsorb light.

Before testing materials in both rigs, blank tests were performed without either reagents, or light or catalyst. In none of these cases, products formation was observed, indicating that catalyst and reagents are stable in reaction conditions and that also in all conditions no photochemical reaction occurs and only the photocatalytic process can be observed and measured.

In performed tests, neither heating nor cooling was used. UV lamp provides a stable and constant temperature of 40 °C on the photocatalytic surface. Afterwards, a gaseous mixture of CO_2 and H_2O was introduced into the reactor. Compressed CO_2 (99.99%) was regulated by a mass flow controller, which was carried through a water bubbler kept at 40 °C to generate CO_2 and H_2O vapour mixture with a 0.07 H_2O/CO_2 molar ratio according to *Equation 2*:

$$H_2O\ flow = \frac{\left(H_2O_{vapour\ pressure}\right)_{T,p} \cdot CO_2 flow}{p_{TOT} - \left(H_2O_{vapour\ pressure}\right)_{T,p}}$$

Equation 2

The reactor was sealed when the reagents ratio was constant. This point was taken as the beginning of the reaction. Therefore, the reaction was performed in static batch conditions. A total of 9.2 μmol of CO_2 and 0.7 μmol of H_2O were present within the sealed reactor.

The reaction products were analysed by a gas chromatograph (HP G1540A) equipped with a Porapak Q column with a TCD detector. Activity results are expressed in turn over numbers (TONs) in $\mu mol \cdot g_{cat}^{-1}$, as commonly used in literature [48, 49]. Photonic yield (Φ) was calculated according to IUPAC recommendations, as the ratio between required electrons for CO_2 reduction to CH_4 (which is considered equal to 8 times CH_4 production) and incident photons [38]:

$$\Phi\ (\%) = \frac{required\ e^- = 8\ \cdot CH_4(mol)}{incident\ photons\ (Einstein)} \cdot 100$$

Equation 3

$$\Phi\ (\%) = \frac{8 \cdot CH_4(mol) \cdot Irr\ (W \cdot m^{-2}) \cdot t\ (s) \cdot A\ (m^2) \cdot \lambda\ (m) \cdot N_A(mol^{-1})}{h\ (J \cdot s) \cdot c\ (m \cdot s^{-1})} \cdot 100$$

Equation 4

where: 8 is the number of required electrons for CO_2 reduction to CH_4, Irr is the irradiance, t is reaction time, A is the illuminated area, λ radiation wavelength, N_A is Avogadro's number, h is Planck's constant and c is speed of light.

DOE experimental conditions were established for the different tests to be carried out at varying reaction times (4, 6 or 8 hours) and irradiance values (40, 50 or 60 $W \cdot m^{-2}$) (see Table 1). First four tests represent the corner points of the model, whereas the last three are the centre points. Test at centre point conditions was performed three times to test the repeatability of the experimental conditions. Experimental ranges for reaction time and irradiance were chosen as centre point conditions used for materials screening.

Table 1 *DOE experimental conditions varied during low irradiance tests.*

Std. Order	Time (h)	Irradiance ($W \cdot m^{-2}$)	Photons (Einstein)
1	4	60	0.011
2	8	60	0.021
3	8	40	0.014
4	4	40	0.007
5	6	50	0.013
6	6	50	0.013
7	6	50	0.013

2.4 Photoactivity tests at high irradiance

High irradiance CO_2 photoreduction with H_2O tests were performed in a cylindrical Pyrex glass reactor (Figure 2), which consisted of two stainless steel lids (one of which was equipped with a quartz window) and a cylindrical Pyrex vessel (diameter 5.5 cm, length 11 cm), which was sealed with O-rings four stainless steel rods secured with wing nuts. The catalyst (20 mg) was suspended in 2-propanol (1 mL) and then deposited on a quartz plate until complete evaporation, keeping the impregnated area equal to 12 cm^2 (width 2 cm, length 6 cm). The impregnated plate was dried for one hour at 110 °C to eliminate completely any trace of dispersing agent.

Similar to the low irradiance reactor tests, a saturator was used to introduce water vapour in the gas inlet, monitoring temperature and pressure using a thermocouple and a pressure gauge, respectively. Irradiation was provided by an OmniCure Series 2000 with a 365 nm filter by Lumen Dynamics and irradiance was controlled by UV/Vis OmniCure Radiometer. Reagents and products were detected using a Hyden Analytical Quadrupole Mass Spectrometer (HPR-20 QIC) equipped with both a Faraday cup and secondary electron multiplier detectors. For a quantitative analysis, before any photocatalytic tests, calibration was performed using gas mixture (BOC Industrial Gases) containing 100 ppm of: hydrogen (H_2), oxygen (O_2), methane (CH_4), methanol (CH_3OH), ethane, (C_2H_6), ethylene (C_2H_4), acetaldehyde (CH_3CHO), ethanol (CH_3CH_2OH) and CO_2 in a balance of Argon.

Experimentally, before each test, the catalyst was introduced into the reactor and let overnight under a 1 $mL \cdot min^{-1}$ helium flow to keep surface clean and avoid atmospheric oxygen contamination. CO_2 (99.999 % BOC Industrial Gases) was then introduced into the reactor using a mass flow controller (8 $mL \cdot min^{-1}$) and was saturated with water vapour

by means of a saturator at room temperature. Considering water vapour pressure at room temperature and CO_2 flow rate, the H_2O/CO_2 ratio was equal to 0.5. Once the reactor was filled with the reaction mixture at 1.5 bar, the reactor was closed and the lamp was switched on. For the DOE analysis, irradiance was varied between 60 and 2400 $W \cdot m^{-2}$, whilst reaction time ranged from one to three hours (Table 2). Blank tests were performed as described for the low irradiance tests.

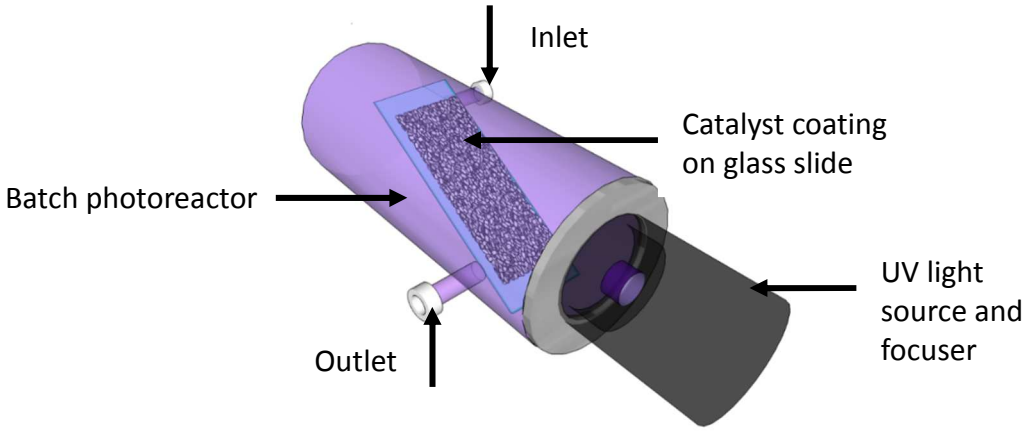

Figure 2 *Batch reactor used for high irradiance experiments.*

Table 2 *DOE experimental conditions varied during high irradiance tests*

Std. Order	Time (h)	Irradiance ($W \cdot m^{-2}$)	Photons (Einstein)
1	1	60	0.008
2	3	60	0.024
3	1	2400	0.316
4	3	2400	0.948
5	2	1200	0.316
6	2	1200	0.316
7	2	1200	0.316

2.5 Statistical analysis of results

For the statistical analysis of data from DOE experiments, Minitab 17 Statistical Software (2010) developed by Minitab, Inc. (PA, USA) [50] was used to create Pareto Charts and assess statistically significant effects of irradiance and reaction time on methane production. Pareto charts of standardised effects and main effects are powerful visualisation tools that summarise the results of the full factorial designs visually. Pareto

charts of standardised effects indicate the statistically significant parameters as those that are above the reference red line. For a parameter to be statistically significant, the null hypothesis of the parameter's co-efficient being equal to zero is tested by comparing the calculated ANOVA *p*-value with a significance test level of $\alpha = 0.05$. If the *p*-value is less than α, the hypothesis that the co-efficient is equal to zero is rejected and deemed to be statistically significant. The weight of the parameters is also indicated by the length of the plotted bar. The main effects plot indicates the parameters effect between its high and low settings. The blue points (Corner point type) on either side of the line are the mean of the values recorded for the high and low settings, where the blue line connects these two points. A line with a steep slope indicates the parameter has a strong effect on the response. The red square indicates the mean of the center points (Center point type), where for this study three replicate points were performed. The grey dotted line indicates the mean for all of the experiments.

3 Results and discussion

3.1 Materials characterisation

The synthesized Au-TiO_2 photocatalyst sample provided suitable surface and lattice properties for CO_2 photoreduction, with similar values to those previously reported in the literature [9, 51, 53]. The N_2 physisorption isotherm (Figure S1) showed this sample is mesoporous and characterised by 110 $m^2 \cdot g^{-1}$ surface area, with wide pore size distribution between 5- 25 nm. The XRD spectrum (Figure S2) concluded that the only titanium dioxide crystal phase observed is anatase, which is the most suitable for photocatalysis, due to its enhanced stability of electron-hole pairs [53]. This experimental evidence is in accordance with UV-Vis spectrum (Figure S3), in which a strong adsorption was observed at wavelengths lower than 388 nm, corresponding to a band gap of 3.21 eV, typical of anatase phase [54]. Moreover, UV-VIS spectrum (Figure S3) shows an absorption between 480 nm and 620 nm relative to gold nanoparticles surface plasmonic resonance, which is correlated to a higher ability to separate surface charges [55].

3.2 Comparison of photoreactor features

The comparison of data collected in the two different rigs, even using the same benchmark material, still represents a challenge [37, 56]. However, there are sufficient similarities that allow to compare the two systems, as reported in Table 3.

Table 3 Comparison of the main features of low and high irradiance rigs.

	Film reactor	Quartz plate reactor
Temperature (°C)	40	25
Pressure (bar)	1	1.5
Catalyst loading per reactor volume (g/cm^3)	0.02	0.00014
Catalyst loading per illuminated area (g/cm^2)	0.001	0.003
H_2O/CO_2 (v/v)	0.07	0.05
Irradiance (W·m^{-2})	40-60	60-2400

It should be noted that in both cases the reaction is performed in a gas-solid system, avoiding mixture issues [57]. Moreover, CO_2 is in excess (H_2O/CO_2 is 0.07 and 0.5 v/v in low and high irradiance rig, respectively) to avoid highly favourable water adsorption and hydrogen production via water splitting, reported in Equation 6 [31, 58].

$$2H_2O \rightleftharpoons 2H_2 + O_2$$

Equation 5

In other terms, the reagents ratio is far above the stoichiometry; from previous studies, a variation of CO_2/H_2O ratio in the range of 0.01 and 0.8, i.e. in large excess of CO_2, does not affect significantly obtained results [59, 60].

$$CO_2 + 2H_2O \rightleftharpoons CH_4 + 2O_2$$

Equation 6

Moreover, in both cases, tests were performed close to atmospheric pressure. According to the Langmuir-Hinshelwood type kinetic model proposed by Tahir and Amin, pressure effect on reaction rate can be considered negligible for low H_2O/CO_2 ratios [61]. Regarding temperature, there are some differences, which might have a beneficial effect on different phenomena, such as reaction kinetics, products desorption and mass transfer [49]. Also the catalyst loading per reactor volume is not similar, affecting diffusion

phenomena; however, preliminary studies excluded diffusion limitations for both reactors [28, 62].

From these considerations, there are fundamental similarities between the two rigs in operative temperature, pressure, catalyst loading and reagents ratio. Nonetheless, there are still several differences in experimental parameters, with the most substantial one being irradiance, which is strictly connected to incident photons, which is the crucial metric for this study.

3.3 Low irradiance DOE tests

For the low irradiance tests, a full factorial design was used to evaluate reaction time (4 – 8 hours) and irradiance (40 – 60 $W \cdot m^{-2}$) as variables on the response of CH_4 production, expressed as methane turnover number (Table 4). In all experiments methane and hydrogen were detected whilst CO, CH_3OH and other hydrocarbons were not observed. This product distribution could be explained by hydrogen being formed from the water splitting reaction and methane by fast CO_2 deoxygenation and following hydrogenation [28], which is the generally desired product in carbon dioxide photoreduction, due to its high H/C ratio.

Table 4 Experimental points and responses used for factorial design of the film reactor.

Std. Order	*Time (h)*	*Irradiance ($W \cdot m^{-2}$)*	*Methane (µmole/g)*	*Hydrogen (µmole/g)*	*Photonic yield CH4 (%)*	*Photonic yield H2 (%)*
1	4	60	20,84	2,80	1,58E-02	2.13E-3
2	8	60	28,50	3,70	1,08E-2	1,40E-3
3	8	40	20,94	3,94	1,19E-2	2,24E-3
4	4	40	12,69	1,54	1,45E-2	1,74E-3
5	6	50	19,49	3,49	2,47E-02	4,416E-
6	6	50	17,34	2,62	2,19E-02	3,315E-
7	6	50	21,04	2,54	2,66E-02	3,214E-

Results reported in Pareto charts (Figure 3) show standardised effects for both irradiance and reaction time on methane production. Both time (p = 0.014) and irradiance (p = 0.014) have a statistically significant effect on methane productivity. No interaction effect between the two variables was found, indicating that they are not dependent on each other. The main effects plot (Figure 4) showed the strong effect of reaction time and irradiance on the production of methane. Equation 7 shows the linear model that only includes statistically significant terms (p<0.05).

$$CH_4 = -10.83 + (1.98 \cdot Time) + (0.392 \cdot Irradiance)$$

Equation 7

where: CH_4 is the yield of methane in μmol·g_{cat}^{-1}, $Time$ is the reaction time in hours and $Irradiance$ is the reaction irradiance in W·m^{-2}.

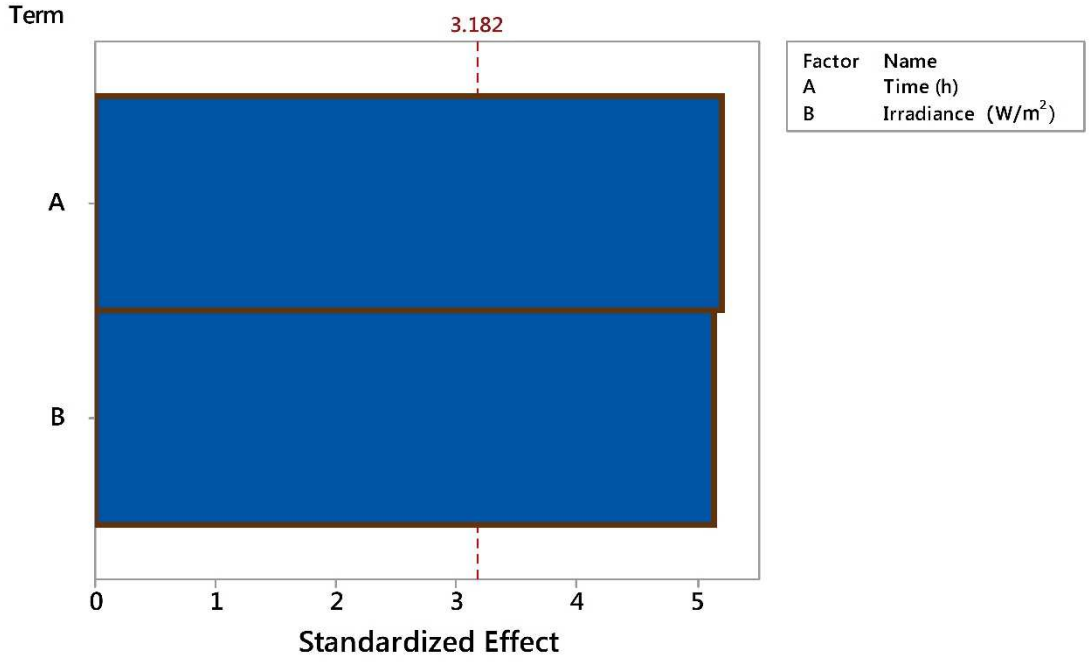

Figure 3 *Pareto Charts for reaction time and irradiance on methane production from the low irradiance DOE tests. Response is methane production in μmol·g_{cat}^{-1}, α=0.05.*

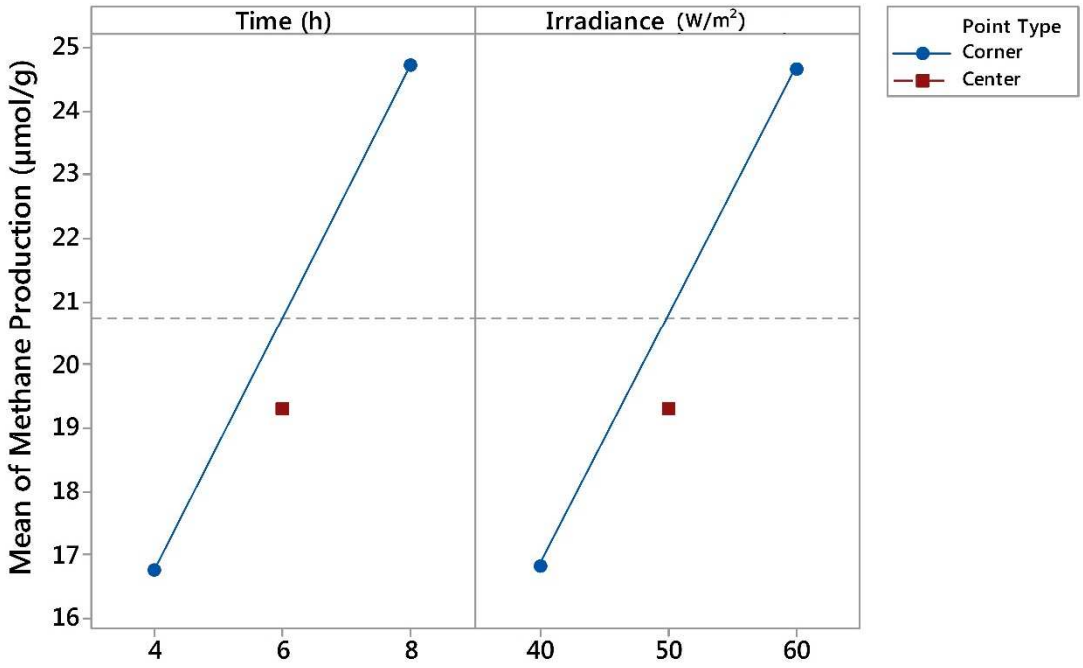

Figure 4 *Main effects plot of reaction time and irradiance on methane production results from low irradiance DOE tests.*

The methane production is represented in a 3-D space as a function of irradiance and reaction time (Figure 5), showing all experimental points are in a plane with a 0.92 R correlation value, confirming that methane production is linearly dependent on both reaction time and irradiance and that these two parameters are independent one to the other on the final output.

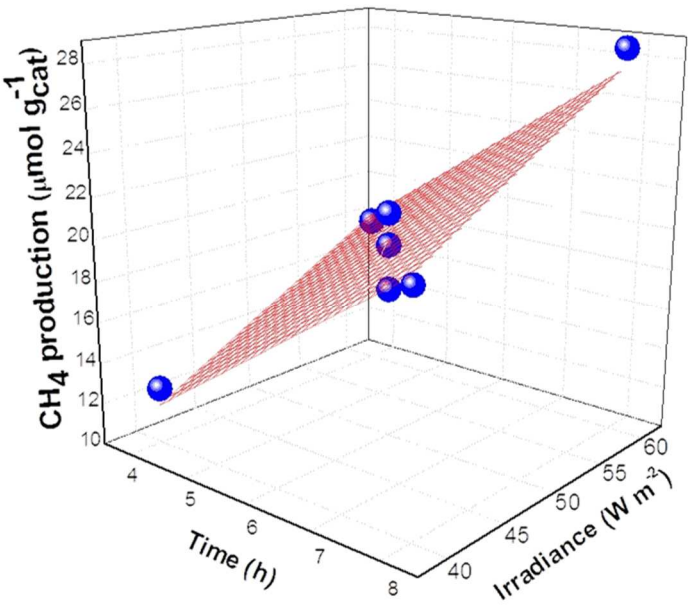

Figure 5 *3-D plot of methane production vs. time and irradiance.*

Considering that incident photons are proportional to both reaction time and irradiance, the overall effect of photonic input on methane formation was considered. Figure 6 shows that methane production is linear with photons input, as assured by R value, regardless of irradiance or reaction time.

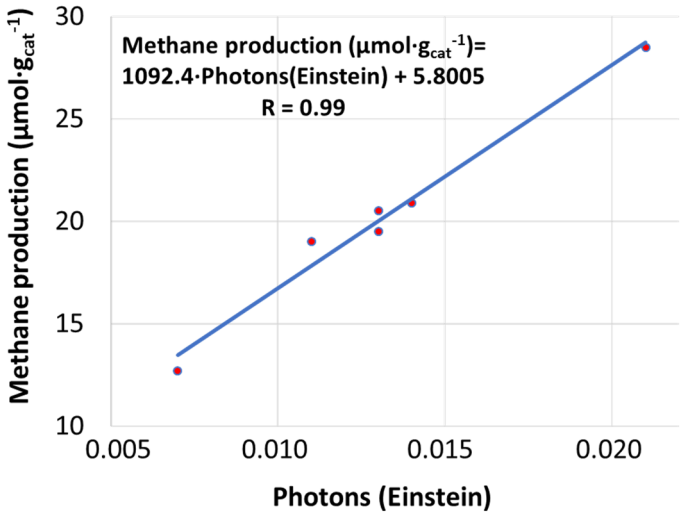

Figure 6 *Methane production as a function of photons input at low irradiance.*

Therefore, at low irradiance methane production by CO_2 photoreduction can be enhanced by increasing irradiance and/or lengthening reaction time, opening to different strategies to pursue this aim. This statistical result from collected data has several implications that explain the effect of photonic input on CO_2 photoreduction. The effect of irradiance observed here is in agreement with previous work by Hermann [37] regarding photocatalytic oxidations. His work indicates that for irradiances lower than a critical value, products formation is proportional to photons input, while higher irradiances might affect recombination rate.

For a deeper understanding of this result, proposed CO_2 photoreduction reaction mechanism should be considered. Photons are explicitly expressed in the first step of the whole process, i.e. photocatalyst activation *via* electrons promotion from valence band (VB) to conduction band (CB).

$$TiO_2 + h\nu \rightarrow h^+ + e^-$$

Equation 8

If photons are considered as proper reactants in the process, it is possible to state that, in these conditions, catalyst photoexcitation is the limiting step of the whole process [28]. This means that, using low irradiances, it is possible to assess whether a material is efficient in light harvesting or not.

In this field, this reported result is particularly relevant because, up to now, irradiance effect has not been thoroughly investigated for CO_2 photoreduction. At the best of author's knowledge, only Tan *et al.* reported the effect of irradiance on methane formation in CO_2 photoreduction with water [21] and observed that methane production increased with irradiance (650 and 1800 $W \cdot m^{-2}$), a range that is significantly higher than values used in this work; however, increase in methane formation was not linear with irradiance and a correlation between them was not reported nor attempted. Therefore, the work presented here represents the first study that assesses the effect of irradiance on CO_2 photoreduction to methane.

Considering reaction time studies in this work, methane production linearly increases with time in the investigated range and no sign of activity loss in methane production with time was observed. In contrast, Bazzo and Urawaka reported CO_2 photoreduction tests at higher temperatures (80 °C and 150 °C) observing an increase in methane production for relatively short reaction times (60 to 90 minutes) following further deactivation [63]. Similar results were found also by Tan *et al.* [64] and Anpo and co-workers [65]. Therefore, it is probable that the experimental reaction time range in this work covers a time region where no (or little) deactivation occurs.

3.4 High irradiance DOE tests

High irradiance tests were performed using a full factorial design, where reaction time (1 – 3 h) and incident irradiance (60 – 2400 $W \cdot m^{-2}$) were evaluated as variables on the response of methane production (Table 5).

The results, reported in Pareto charts (Figure 7), show standardised effects for both irradiance and reaction time on methane production. Reaction time (p = 0.048) is a statistically significant effect on methane productivity. No interaction effect between the two variables was found, indicating that they are not dependent one to the other. The main effects plot (Figure 8) showed the strong effect of reaction time on the production of methane. Conversely, irradiance is much weaker effect and statistically insignificant (Figure 8). Equation 9 shows the linear model that only includes statistically significant terms (p<0.05):

$$\boldsymbol{CH_4 = -9.78 \cdot 10^{-2} + (0.126 \cdot Time)}$$

Equation 9

where: $\boldsymbol{CH_4}$ is the yield of methane in μmol·g_{cat}^{-1} and $\boldsymbol{Time}$ is the reaction time in hours.

Table 5 *Experimental points and responses used for factorial design collected using quartz plate reactor.*

Std. Order	Time (h)	Irradiance ($W \cdot m^{-2}$)	Methane (μmol·g_{cat}^{-1})	Hydrogen (μmole/g)	Photonic yield CH4 (%)	Photonic yield H2 (%)
1	1	60	$4.43 \cdot 10^{-3}$	1,30E-02	1,59E-03	1,83E-02
2	3	60	$3.05 \cdot 10^{-1}$	9,00E-01	3,30E-02	3,88E-01
3	1	2400	$7.08 \cdot 10^{-2}$	2,10E-01	2,15E-04	2,57E-03
4	3	2400	$2.74 \cdot 10^{-1}$	8,00E-01	2,50E-03	2,91E-02
5	2	1240	$6.64 \cdot 10^{-2}$	1,90E-01	1,21E-03	1,39E-02
6	2	1240	$1.90 \cdot 10^{-1}$	5,70E-01	3,23E-04	3,88E-03
7	2	1240	$1.77 \cdot 10^{-2}$	6,00E-02	3,47E-03	3,99E-02

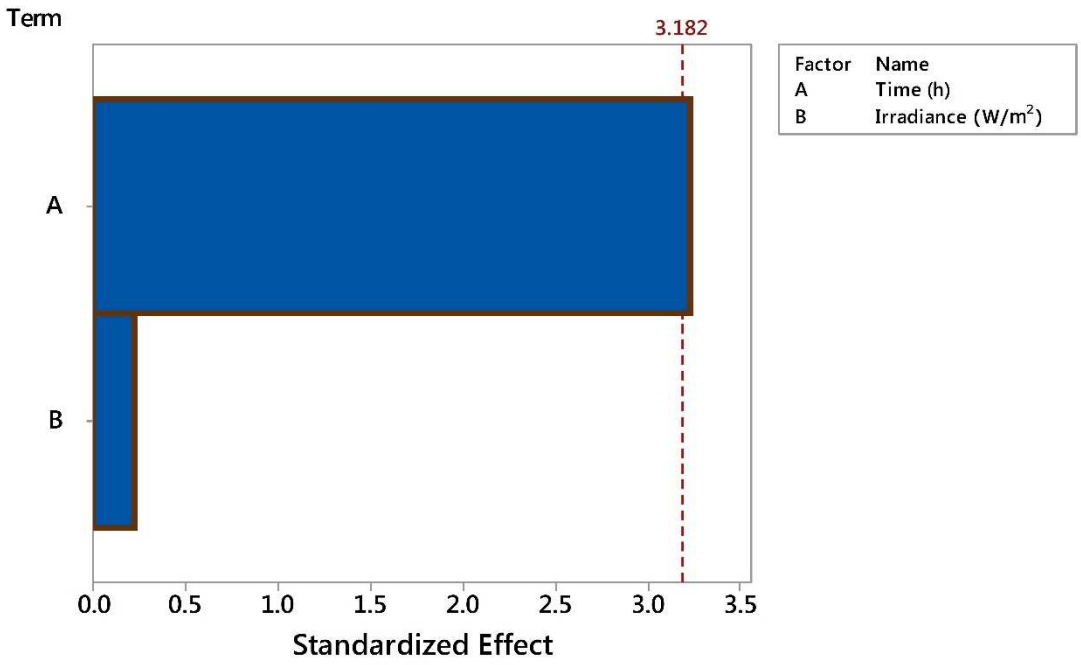

Figure 7 *Pareto Charts from ANOVA analysis of results from high irradiance DOE tests. Response is methane production in* $\mu mol \cdot g_{cat}^{-1}$, $\alpha=0.05$.

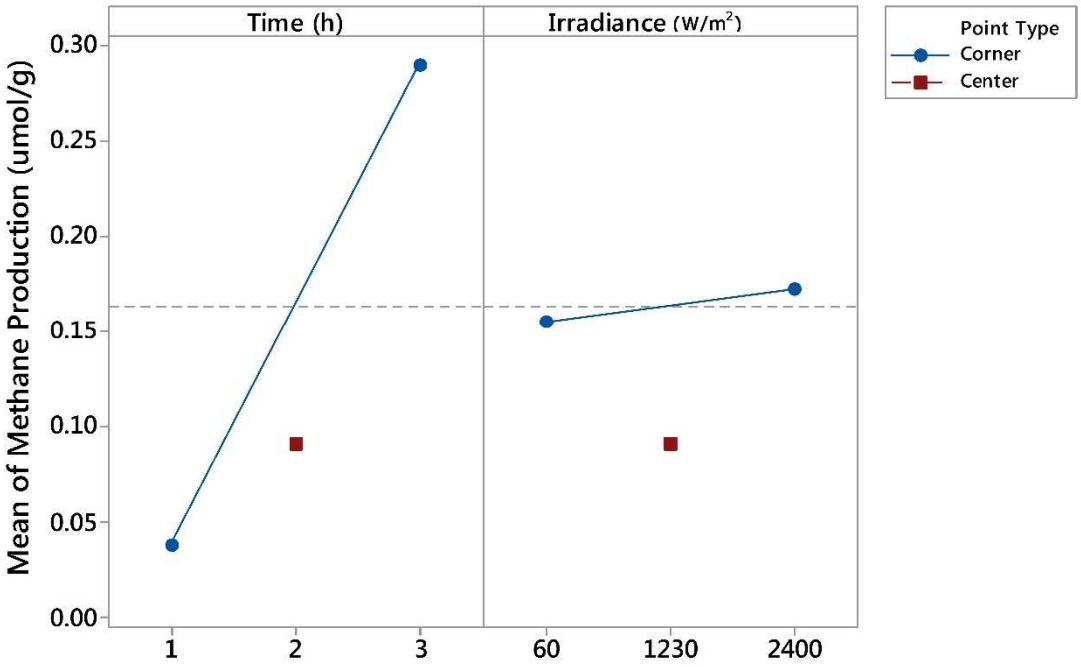

Figure 8 *Main effects plot of reaction time and irradiance on methane production results from high irradiance DOE tests.*

The trends observed for high irradiance are different from those observed at low irradiances, where both reaction time and irradiance were significant parameters. In fact,

in these reaction conditions, time effect on photonic input is consistently more significant than irradiance, which is almost negligible within the investigated experimental range.

The small significance of irradiance on CH_4 formation can be explained considering that, in this experimental range, a small fraction of incident photons is able to activate all available photocatalytic sites, and therefore, a further increase in photonic input does not provide an increase in methane formation.

The effect of irradiance on CO_2 photoreduction was reported only by Tan and co-workers [21] but a correlation between products formation and irradiance has not been reported yet, so some comparisons must be made with more established photooxidative processes. For example, Vorontsov and Dubovitskaya reported that ethanol photocatalytic oxidation rate reached a steady state for high irradiance, thus not being a significant parameter for the process [66]. This phenomenon was also observed for toluene and formaldehyde oxidation by Strini and Schiavi [67] and Ching and co-workers [68], respectively. From this comparison with available papers on photooxidations, it is possible to sustain proposed explanation for irradiance irrelevance in these conditions, since they allow to saturate photocatalytic surface with photons already.

For a deeper understanding of this result, it is not possible to consider, like in low irradiance tests, TiO_2 photoexcitation and therefore, it should be assumed that photoactivation is not the limiting determining step of the overall process. The surface chemical reaction has proven to be a particularly difficult step in the overall process. In particular, as proposed by Tan et al., binding CO_2 adsorption on TiO_2 proved to be a particularly delicate, especially on TiO_2 [21].

$$\boldsymbol{CO_2 \xrightarrow{cat} CO_{2,\ ads}} \qquad \textit{Equation 10}$$

$$\boldsymbol{CO_{2,ads} \xrightarrow{cat} C^*_{ads} + O_2} \qquad \textit{Equation 11}$$

$$\boldsymbol{H_2O \xrightarrow{cat} H^*_{ads} + OH^*_{ads}} \qquad \textit{Equation 12}$$

$$\boldsymbol{OH^*_{ads} \xrightarrow{cat} H^*_{ads} + {}^1\!/_2\, O_2} \qquad \textit{Equation 13}$$

$$\boldsymbol{C^*_{ads} + 4H^*_{ads} \xrightarrow{cat} CH_{4,ads}} \qquad \textit{Equation 14}$$

$$\boldsymbol{CH_{4,ads} \xrightarrow{cat} CH_4} \qquad \textit{Equation 15}$$

Therefore, high irradiance conditions are suitable to assess whether a material is effective in surface catalytic CO_2 reduction or not.

Considering together results at low and high irradiance, it is possible to assess whether a material is more efficient in photoexcitation or in the catalytic reaction itself. In the case of considered material, i.e. Au/TiO_2, catalyst activation by photons is faster than reagents conversion to reagents. The coupling of low and high irradiance tests allowed to assess the strength of investigated material and suggest ways to improve it, i.e. by enhancing reagents interaction with the catalyst.

Conclusions

Assessing irradiance conditions is fundamental to understand results from photocatalytic CO_2 reduction. Photons represent the primary energetic input and a change in this parameter might have an effect on materials performance.

The different effect of photonic input was assessed by design of experiments approach, considering the experimental parameters affecting photons input, i.e. irradiance and reaction time. The effect of these variables proved to be different according to experimental regimes. At low irradiance, where surface is not saturated with photons, both reaction time and irradiance proved to influence significantly methane production, indicating that photoexcitation limits overall process efficiency. On the contrary, ~~whereas~~, at high irradiance, due to photonic saturation of the surface, irradiance increase does not affect photocatalytic performance, but prolonged time proved to be important to increase methane yield, allowing to investigate CO_2 conversion itself. Therefore, a single irradiance condition is not sufficient to assess materials activity, but, to handle a more comprehensive understanding of materials behaviours, low irradiance tests, which indicate materials photoactivity, should be couples to high irradiance one, show how efficiently the catalyst interacts with reagents.

Acknowledgements

The authors thank Tania Fantinel (Ca' Foscari University Venice) and Richard Kinsella (Heriot-Watt University) for the excellent technical assistance. The authors acknowledge EU ERASMUS + Traineeship program for support of the collaboration between Research Centre for Carbon Solutions (RCCS) at Heriot Watt University and the Department of Molecular Sciences and Nanosystems at Ca' Foscari University Venice. The authors also thank the financial support provided by the Engineering and Physical Sciences Research Council (EP/K021796/1), the Research Centre for Carbon Solutions (RCCS) and the James Watt Scholarship Programme at Heriot-Watt University. We are also grateful for

the support provided by the Heriot-Watt Buchan Chair in Sustainable Energy Engineering.

References

1.K. Li, X. An, K. Park, M. Khraisheh, Y. Tang, Catalysis Today 224 (2014) 3-12.

2 C. Peng, G. Reid, H.F. Wang, P. Hu, Journal of Chemical Physics 147 (2017) 30901-1,30901-14.

3 O. Ola, M. Maroto-Valer, Journal of Photochemistry and Photobiology C: Photochemistry Reviews 24 (2015) 16-42.

4 D. Chen, X.G. Zhang, A.F. Lee, Journal of Materials Chemistry A 3 (2015) 14487-14516.

5 Y.C. Chen, J. Jiao, Z, Zhao, W. Zhong, J. Li, J. Liu, G. Jiang, A. Duan, Journal of Materials Chemistry A 3 (2015) 11074-11085.

6 S. Ijaz, M.F. Ehsan, M.S. Ashiq, N. Karamat, T. He, Applied Surface Science 390 (2016) 550-559.

7 J. Yu, J. Jin, B. Cheng, M. Jaroniec, Journal of Materials Chemistry A 2 (2014) 3407-3416.

8 K.L. Bae, J. Kim, C.K. Lim, K.M. Nam, H. Song, Nature Communications, 2017 in press doi:10.1038/s41467-017-01165-4.

9 L. Collado, P. Jana, B. Sierra, J.M. Coronado, P. Pizarro, D.P. Serrano, V. De la Peña O'Shea, Chemical Engineering Journal 224 (2013) 128-135.

10 T. Sukonket, A. Khan, B. Saha, H. Ibrahim, S. Tantayanon, P. Kumar, R. Idem, Energy & Fuels 25 (2011) 864-877.

11 F. Riboni, L.G. Bettini, D.W. Bahnemann, E. Selli, Catalysis Today 209 (2013) 29-34.

12 Y. Bi, M. Fahad Ehsan, Y. Huang, J. Jin, T. He, Journal of CO_2 Utilization 12 (2015) 43-48.

13 J. Schneider, M. Matsuoka, M. Takeuchi, J. Zhang, Y. Horiuchi, M. Anpo, D.W. Bahnemann, Chemical Reviews 114 (2014) 9919-9986.

14 Y. Ma, X. Wang, Y. Jia, X. Chen, H. Han, C. Li, Chemical Reviews 114 (2014) 9987-10043.

15 E. Karamian, S. Sharifnia, Journal of CO_2 Utilization 16 (2016) 194-203.

16 J. Highfield, Molecules 20 (2015) 6739-6793.

17 Z. Jiang, D. Ding, L.J. Wang, Y.X. Zhang, L. Zan, Catalysis Science and Technology 14 (2017) 3065-3072.

18 A.D. Handoko, K.F. Li, J.W. Tang, Current Opinions in Chemical Engineering 2 (2013) 200-206.

19 J. Choi, H. Park, M.R: Hoffmann, Journal of Physical Chemistry C 114 (2010)783-792.

20 M.E. Aguirre, R. Zhou, A.J. Eugene, M.I. Guzman, M.A. Grela, Applied Catalysis B: Environmental

21 L.L. Tan, W.J. Ong, S.P. Chai, A.R. Mohamed, Chemical Engineering Journal, 308 (2017) 248-255.

22 A. Ayati, A. Ahmadpour, F.F. Bamoharram, B. Tanhaei, M. Mänttäri, S. Sillanpää, Chemosphere 107 (2014) 163-174.

23 M. Tahir, Applied Catalysis B: Environmental 219 (2017) 329-343.

24 M.L. Ovcharov, V.V. Shvalagin, V.M. Gran Chak, Theoretical and Experimental Chemistry 50 (2014) 53-58.

25 S. Das, W. Wan Daud, Renewable and Sustainable Energy Reviews 39 (2014) 765-805.

26 M. Tahir, N. Amin, Renewable and Sustainable Energy Reviews 25 (2013) 560-579.

27 A. Olivo, D. Zanardo, E. Ghedini, F. Menegazzo, M. Signoretto, Chemengineering 2 (2018) 42-75.

28 A. Olivo, E. Ghedini, M. Signoretto, M. Compagnoni, I. Rossetti, Energies 10 (2017) 1394-1407.
29 H. Kawanami, D.C. Grills, T. Ishizaka, M. Chatterjee, A. Suzuki, Journal of CO_2 Utilization 3-4 (2013) 93-97.
30 P. Richardson, M. Perdigoto, W. Wang, R.J.G. Lopes, Applied Catalysis B. Environmental 132-133 (2013) 408-415.
31 L. Liu, F. Gao, H. Zhao, Y: Li, Applied Catalysis B: Environmental 134-135 (2013) 349-358.
32 M. Tahir, N. Amin, Applied Catalysis B: Environmental 162 (2015) 98-109.
33 B. Michalkiewicz, J. Majewska, G. Kasziolka, K. Bubacz, S: Mozia, A.W. Morawski, Journal of CO_2 Utilization 5 (2014) 47-52.
34 M. Tahir, B. Tahir, N. Amin, Chemical Engineering Transactions 56 (2017) 319-324.
35 T.V. Nguyen, J.C.S. Wu, Applied Catalysis A: General 335 (2008) 112-120.
36 Y. Wang, B. Li, C. Zhang, L. Cui, S. Kang, X. Li, L. Zhou, Applied Catalysis B: Environmental 130-131 (2013) 277-284.
37 J.M. Hermann, Applied Catalysis B: Environmental 99 (2010) 461-468.
38 S.E. Braslavsky, A.M. Braun, A.E. Cassano, A.V. Emeline, M.I. Litter, L. Palmisano, V.N. Parmon, N. Serpone, Pure and Applied Chemistry 83 (2011) 931-1014.
39 J. Antony, Design of Experiments for Engineers and Scientists, 1st ed., Elsevier Science, Amsterdam, 2014.
40 W.A. Thompson, C. Perier, M.M. Maroto-Valer, Applied Catalysis B: Environmental 238 (2018) 136-146.
41 W.A. Thompson, A. Olivo, D. Zanardo, G. Cruciani, F. Menegazzo, M. Signoretto, M.M. Maroto-Valer, RSC Advances 9 (2019) 21660-21666.
42 M.A. Tabatabai, Environmental Letter 7 (1974) 237-243.
43 R. Zanella, S. Giorgio, C.R. Henry, C. Louis, Journal of Physical Chemistry B 106 (2002) 7634-7642.
44 F. Menegazzo, M. Signoretto, F. Pinna, M. Manzoli, V. Aina, G. Cerrato, B. Flora, Journal of Catalysis 309 (2014) 241-247.
45 F.E. Clarke, Analytical Chemistry 4 (1950) 553-555.
46 S. Brunauer, P.H. Emmett, E. Teller, Journal of American Chemical Society 60 (1938) 309-319.
47 E.P. Barrett, L.S. Joyner, P.P. Halenda, Journal of American Chemical Society 73 (1951) 373-380.
48 D. Liu, Y. Fernandez, O. Ola, M. Maroto-Valer, C.M.A. Parlett, A.F. Lee, J.C.S Wu, Catalysis Communication 25 (2012) 78-82.
49 M. Tahir, N.S. Amin, Applied Catalysis B: Environmental 142-143 (2013) 512-522.
50 Minitab Inc. Official Website: https://www.minitab.com.
51 M. Tahir, Applied Catalysis B: Environmental 219 (2017) 329-343.
52 A. Olivo, E. Ghedini, P. Pascalicchio, M. Manzoli, G. Cruciani, M. Signoretto, Catalysts 8 (2018) 41-61.
53 M. Janus, M. Inagaki, B. Tryba, M. Toyoda, A.W. Morawski, Applied Catalysis B: Environmental 63 (2006) 272-276.
54 K. Nagaveni, M.S. Hedge, N. Ravishankar, G.N. Subbana, G. Madras, Langmuir 20 (2004) 2900-2907.
55 L. Devi, R. Kavitha, Applied Catalysis B: Environmental 140-141 (2013) 559-587.
56 S. Neatu, J. Macià-Agullò, H. Garcia, International Journal of Molecular Sciences 15 (2014) 5246-5262.

57 P.L. Richardson, M.L.N. Perdigoto, W. Wang, R.J.G. Lopes, Applied Catalysis B: Environmental 132-133 (2013) 408–415.
58 A. Olivo, V. Trevisan, E. Ghedini, F. Pinna, C.L. Bianchi, A. Naldoni, G. Cruciani, M. Signoretto, Journal of CO_2 Utilization 12 (2015) 86-94.
59 Y. Li, Y. Luo, ACS Catalysis 6 (2016) 2018-2015.
60 V. Vaiano, D. Sannino, P. Ciambelli, Chemical Engineering Transactions 43 (2015) 1003-1008.
61 M. Tahir, N. Amin, Chemical Engineering Journal 230 (2013) 314-327.
62 O. Ola, M. Maroto-Valer, Applied Catalysis A: General 502 (2015) 114-121.
63 A. Bazzo, A. Urawaka, ChemSusChem 6 (2013) 2095-2102.
64 J. Tan, Y. Fernàndez, D. Liu, M. Maroto-Valer, J. Bian, X. Zhang, Chemical Physics Letters 531 (2012) 149-154.
65 M. Anpo, H. Yamashita, Y. Ichihashi, S. Ehara, Journal of Electroanalytical Chemistry 396 (1995) 21-26.
66 A.V. Vorontsov, V.P. Dubovitskaya, Journal of Catalysis 221 (2004) 102-109.
67 A. Strini, L. Schiavi, Applied Catalysis B: Environmental 103 (2011) 226-231.
68 W.H. Ching. M. Leung, D.Y.C. Leung, Solar Energy 77 (2004) 129-135.